

Tunable optomechanically induced transparency and fast-slow light in a loop-coupled optomechanical system

Qinghong Liao(廖庆洪), Xiaoqian Wang(王晓倩), Gaoqian He(何高倩), and Liangtao Zhou(周良涛)
Citation: Chin. Phys. B, 2021, 30 (**9**): 094205. DOI: 10.1088/1674-1056/ac0cda
Journal homepage: http://cpb.iphy.ac.cn; http://iopscience.iop.org/cpb

What follows is a list of articles you may be interested in

Controllable four-wave mixing response in a dual-cavity hybrid optomechanical system

Lei Shang(尚蕾), Bin Chen(陈彬), Li-Li Xing(邢丽丽), Jian-Bin Chen(陈建宾), Hai-Bin Xue(薛海斌), and Kang-Xian Guo(郭康贤)
Chin. Phys. B, 2021, 30 (**5**): 054209. DOI: 10.1088/1674-1056/abd695

Effects of the Casimir force on the properties of a hybrid optomechanical system

Yi-Ping Wang(王一平), Zhu-Cheng Zhang(张筑城), Ya-Fei Yu(於亚飞), Zhi-Ming Zhang(张智明)
Chin. Phys. B, 2019, 28 (**1**): 014202. DOI: 10.1088/1674-1056/28/1/014202

Optomechanically induced transparency with Bose–Einstein condensate in double-cavity optomechanical system

Li-Wei Liu(刘利伟), Duo-Jie Gengzang(更藏多杰), Xiu-Jia An(安秀加), Pei-Yu Wang(王培煜)
Chin. Phys. B, 2018, 27 (**3**): 034205. DOI: 10.1088/1674-1056/27/3/034205

Controllable double electromagnetically induced transparency in a closed four-level-loop cavity–atom system

Miao-Di Guo(郭苗迪), Xue-Mei Su(苏雪梅)
Chin. Phys. B, 2017, 26 (**7**): 074207. DOI: 10.1088/1674-1056/26/7/074207

Adjustable quantum coherence effects in a hybrid optomechanical system

Wen-Qing Xia(夏文清), Ya-Fei Yu(於亚飞), Zhi-Ming Zhang(张智明)
Chin. Phys. B, 2017, 26 (**5**): 054210. DOI: 10.1088/1674-1056/26/5/054210

Tunable optomechanically induced transparency and fast–slow light in a loop-coupled optomechanical system*

Qinghong Liao(廖庆洪)[1,2,†], Xiaoqian Wang(王晓倩)[1], Gaoqian He(何高倩)[1], and Liangtao Zhou(周良涛)[1]

[1] *Department of Electronic Information Engineering, Nanchang University, Nanchang* 330031, *China*
[2] *Key Laboratory of Opto-Electronic Information Acquisition and Manipulation of Ministry of Education, Anhui University, Hefei* 230601, *China*

(Received 14 April 2021; revised manuscript received 3 June 2021; accepted manuscript online 21 June 2021)

We theoretically explore the tunability of optomechanically induced transparency (OMIT) phenomenon and fast–slow light effect in a loop-coupled hybrid optomechanical system in which two optical modes are coupled to a common mechanical mode. In the probe output spectrum, we find that the interference phenomena OMIT caused by the optomechanical interactions and the normal mode splitting (NMS) induced by the strong tunnel coupling between the cavities can be observed. We further observe that the tunnel interaction will affect the distance and the heights of the sideband absorption peaks. The results also show that the switch from absorption to amplification can be realized by tuning the driving strength because of the existence of stability condition. Except from modulating the tunnel interaction, the conversion between slow light and fast light also can be achieved by adjusting the optomechanical interaction in the output field. This study may provide a potential application in the fields of high precision measurement and quantum information processing.

Keywords: hybrid optomechanical system, optomechanically induced transparency and absorption, normal mode splitting, fast light and slow light

PACS: 42.50.–p, 42.50.Nn, 42.50.Ct, 42.50.Md **DOI:** 10.1088/1674-1056/ac0cda

1. Introduction

A cavity optomechanical system (COMS),[1,2] which describes the interaction between the mechanical resonator and the light via radiation pressure, has brought significant development in many different areas of physics. It is widely acknowledged that the COMS possesses diverse potential applications, such as quantum entanglement,[3,4] NMS,[5–7] ground-state cooling of mechanical modes,[8–11] electromagnetically induced transparency (EIT),[12–17] and optomechanically induced absorption (OMIA)[18] phenomena, *etc*. To a large extent, it promotes the development of photon transmission and quantum information processing. OMIT is a typical example of light-control light via mechanical motion.[5,19,20] Analogous to EIT, the OMIT resulting from the destructive interference of the anti-Stokes scattering field and the weak probe field plays an essential part in quantum information and communication processes.[21–24] In theory Agarwal and Huang have discovered that the optomechanical system becomes transparent to a weak detection field at resonant point when a strong pump field is applied to drive the optical cavity.[25–27] Furthermore, it has been also sequentially confirmed in experiments[28,29] and has received much attention in a hybrid COMS,[27] a quadratically coupled COMS,[26–30] a spinning COMS,[31] and in a parity-time symmetric microcavity system,[32,33] *etc*. Physically the phenomena of OMIA is also predicted in a hybrid optomechanical system.[18]

Due to the narrow transparency window accompanying with the abnormal dispersion, the most outstanding application of OMIT is considered as storage and light delay.[34–37] In the last few years, what has interested us extremely is the study on fast–slow light effect.[38–41] Various techniques have been developed to realize fast–slow light. One method is the use of the EIT technology, a quantum interference effect that can produce the dramatic change of the absorption and dispersion properties. Thus, the nonlinear susceptibility is enhanced and slow light is generated.[42,43] Akram *et al*.[44] have studied the fast and slow light effects in a hybrid COMS based on EIT technology. Another application among these ways is to control the group delay τ of light pulses,[45] resulting in slow light ($\tau > 0$) and fast light effects ($\tau < 0$). Many schemes for studying fast–slow light have been proposed in the COMS. For instance, Zhan *et al*.[43] have observed that slow light can be achieved over an extensive range of parameters even at high temperature such as 200 K in a quadratically coupled COMS. Akram *et al*.[44] have found that adding atom–field coupling into the hybrid system can further enhance the fast light effect obtained by single optical-mechanical coupling. Additionally, the conversion between fast light and slow light has been done under the action of an external force.[46] It is reported that the

*Project supported by the National Natural Science Foundation of China (Grant No. 62061028), the Foundation for Distinguished Young Scientists of Jiangxi Province, China (Grant No. 20162BCB23009), the Open Research Fund Program of the State Key Laboratory of Low-Dimensional Quantum Physics (Grant No. KF202010), the Interdisciplinary Innovation Fund of Nanchang University (Grant No. 9166-27060003-YB12), and the Open Research Fund Program of the Key Laboratory of Opto-Electronic Information Acquisition and Manipulation of Ministry of Education (Grant No. OEIAM202004).

†Corresponding author. E-mail: nculqh@163.com

© 2021 Chinese Physical Society and IOP Publishing Ltd

transmitted probe beam can be delayed as much as 4 μs and can be easily controlled by the power of the pump beams in a two-mode COMS.[47] More recently, Macke *et al.*[48] have found that both slow and fast light can be obtained by selecting particular phase components of the transmitted field in a zero-dispersion configuration. And Chen *et al.*[49] have observed that a tunable and controllable fast-to-slow light propagation can be achieved by controlling the driving amplitudes and phase of the phonon pump. In parallel, the research of the multiple-mode optomechanical systems has attracted much attention and many quantum phenomena have been studied in recent years. Xu *et al.*[50] have found that the EPs periodically emerge and the sidebands' spectrum can be modified significantly by tuning the relative positions of the nanotips. Hao *et al.*[51] have indicated that the controllable amplification of the probe light can be achieved, which is induced by the constructive interactions of photon, atom, and phonon. It has been determined that tuning the OPA parameters can considerably suppress quantum back-action noise and enable the device to reach sub-SQL sensitivity.[52] Furthermore, the sensitive impacts of the dark mode effect on the optical properties in a three-mode loop-coupled optomechanical system have been proposed in Ref. [53]. Besides, Liu *et al.*[54] have investigated the squeezing transfers from a squeezed vacuum injected in one cavity to the output spectrum of the other cavity in the two-cavity optomechanical system. Lai *et al.*[55] have found that the ground-state cooling of the two mechanical resonators can be realized simultaneously under the optimal driving detuning and in the resolved-sideband regime.

Motivated by these developments, we theoretically consider a circular hybrid model,[3,56] where two optical cavities are coupled to a common mechanical resonator identically.[57–59] At the same time, the two optical cavities interact with each other through photon-coupled paths. The present work has the following distinct features: Firstly, the photon coupling strengths and related parameters can be precisely adjusted to realize controllable photon transmission. Secondly, we propose a pump–probe optical method to detect tunnel coupling strength. Thirdly, the conversion between slow light and fast light can be achieved by adjusting a variety of paths, which provides an excellent platform for the modulation of fast light and slow light.

The main research content is as follows: In Section 2 we give out the model of the hybrid COMS considered in our work and calculate the amplitude of the output corresponding to the weak probe analytically. In Section 3, we discuss the OMIT (OMIA) and give the explicit explanation for the mechanism. Furthermore, we study the influence of different factors on OMIT. A conversion between OMIT and OMIA adjusted by related parameters is emphasized. In Section 4, the group delay of the output field is also investigated. Finally, we present our conclusions in Section 5.

2. Theoretical model and solutions

As shown in Fig. 1, the loop-coupled hybrid optomechanical system under consideration here consists of a mechanical resonator coupled to two optical cavities, which are coupled to each other with the tunneling strength J. A strong driving laser with frequency $\omega_{\rm p}$ and field amplitude $E_{\rm p}=\sqrt{2P_{\rm p}\kappa_1/\hbar\omega_{\rm p}}$, and a weak probe laser with frequency $\omega_{\rm r}$ and amplitude $E_{\rm r}=\sqrt{2P_{\rm r}\kappa_1/\hbar\omega_{\rm r}}$ are applied to this system. Here, $P_{\rm p}$ ($P_{\rm r}$) is the pump (probe) light power, and κ_i ($i=1,2$) is the field decay of the i-th optical cavity.[60]

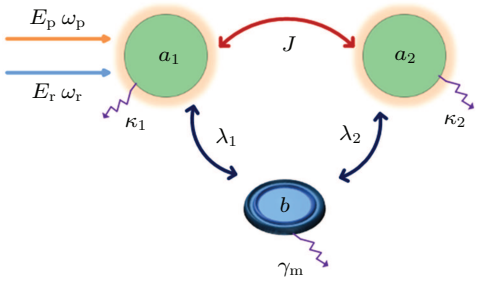


Fig. 1. Schematic diagram of the loop-coupled hybrid optomechanical system composed of two optical cavities coupled to the same mechanical resonator. The two cavities are coupled directly with intercavity coupling strength J. The system is driven by a strong pump laser and a weak probe laser.

Introducing the rotating wave approximation at the pump frequency $\omega_{\rm p}$, the effective Hamiltonian of the system reads[61,62]

$$H=H_0+H_{\rm I}+H_{\rm D}, \tag{1a}$$

$$H_0=\hbar\Delta_1 a_1^{+}a_1+\hbar\Delta_2 a_2^{+}a_2+\hbar\omega_{\rm m}b^{+}b, \tag{1b}$$

$$H_{\rm I}=-\hbar\lambda_1 a_1^{+}a_1Q-\hbar\lambda_2 a_2^{+}a_2Q+J\left(a_1a_2^{+}+a_1^{+}a_2\right), \tag{1c}$$

$$H_{\rm D}={\rm i}\hbar\left(E_{\rm p}a_1^{+}-E_{\rm p}^{*}a_1\right)+{\rm i}\hbar\left(E_{\rm r}a_1^{+}{\rm e}^{-{\rm i}\delta t}-E_{\rm r}^{*}a_1{\rm e}^{{\rm i}\delta t}\right), \tag{1d}$$

with $\delta=\omega_{\rm r}-\omega_{\rm p}$. Here, H_0 represents the free Hamiltonian of the system, where a_i and b are the annihilation operators describing the optical fields and the mechanical resonator, respectively. The frequency of the mechanical resonator is $\omega_{\rm m}$ and $\Delta_i=\omega_{{\rm c}i}-\omega_{\rm p}$ gives the detuning between the cavities ($\omega_{{\rm c}i}$) and the optical drive ($\omega_{\rm p}$) frequencies. The second term $H_{\rm I}$ defines the interaction Hamiltonian. Cavity fields are coupled to the mechanical resonator via the linear optomechanical coupling λ_i ($i=1,2$). J is the coupling strength between the two cavities. The final term $H_{\rm D}$ describes the interaction Hamiltonian between the optomechanical system and the control field as well as the probe field.

Based on the Hamiltonian in Eqs. (1a)–(1d), the Heisenberg equations including the corresponding noise and damping terms can be given by ($\hbar=1$)

$$\begin{aligned}\frac{{\rm d}a_1}{{\rm d}t}=&-({\rm i}\Delta_1+\kappa_1)a_1+{\rm i}\lambda_1 a_1Q\\&-{\rm i}Ja_2+E_{\rm p}+E_{\rm r}{\rm e}^{-{\rm i}\delta t},\end{aligned} \tag{2a}$$

$$\frac{\mathrm{d}a_2}{\mathrm{d}t} = -(\mathrm{i}\Delta_2+\kappa_2)a_2+\mathrm{i}\lambda_2 a_2 Q-\mathrm{i}Ja_1, \tag{2b}$$

$$\frac{\mathrm{d}Q}{\mathrm{d}t} = \mathrm{i}\omega_\mathrm{m}\left(b^+-b\right), \tag{2c}$$

$$\frac{\mathrm{d}^2Q}{\mathrm{d}t^2}+\omega_\mathrm{m}^2 Q+\gamma_\mathrm{m}\frac{\mathrm{d}Q}{\mathrm{d}t} = 2\omega_\mathrm{m}\lambda_1 a_1^+ a_1+2\omega_\mathrm{m}\lambda_2 a_2^+ a_2, \tag{2d}$$

where γ_m is defined as the decay rate of the mechanical resonator. The following ansatz is adopted to solve the Eqs. (2a)–(2b):

$$a_1(t) = a_{10}+a_{1+}\mathrm{e}^{-\mathrm{i}\delta t}+a_{1-}\mathrm{e}^{\mathrm{i}\delta t}, \tag{3a}$$

$$a_2(t) = a_{20}+a_{2+}\mathrm{e}^{-\mathrm{i}\delta t}+a_{2-}\mathrm{e}^{\mathrm{i}\delta t}, \tag{3b}$$

$$Q(t) = Q_0+Q_+\mathrm{e}^{-\mathrm{i}\delta t}+Q_-\mathrm{e}^{\mathrm{i}\delta t}. \tag{3c}$$

Substituting Eqs. (3a)–(3c) into Eqs. (2a)–(2d) and ignoring all the small-terms multiplication as well as the second-order terms, we obtain

$$a_{1+} = \frac{E_\mathrm{r}C_0}{(C_0C_3+J^2)-\dfrac{D_2+D_4J^2+D_5J^4+D_6J^6}{D_1-D_3J^2}}, \tag{4}$$

where

$$\begin{aligned}
&B_1 = \mathrm{i}\eta n_{\mathrm{p}1}a_1\omega_\mathrm{m}, \quad B_2 = \mathrm{i}\eta n_{\mathrm{p}1}a_2\omega_\mathrm{m},\\
&B_3 = \mathrm{i}\eta n_{\mathrm{p}1}a_3\omega_\mathrm{m}, \quad B_4 = \mathrm{i}\eta n_{\mathrm{p}2}a_2\omega_\mathrm{m},\\
&C_0 = -\mathrm{i}\delta+(\mathrm{i}\Delta_2+\kappa_2)-\mathrm{i}\lambda_2 Q_0,\\
&C_1 = -\mathrm{i}\delta-(\mathrm{i}\Delta_1-\kappa_1)+\mathrm{i}\lambda_1 Q_0,\\
&C_2 = -\mathrm{i}\delta-(\mathrm{i}\Delta_2-\kappa_2)+\mathrm{i}\lambda_2 Q_0,\\
&C_3 = -\mathrm{i}\delta+(\mathrm{i}\Delta_1+\kappa_1)-\mathrm{i}\lambda_1 Q_0,\\
&C_4 = -(\mathrm{i}\Delta_2+\kappa_2)+\mathrm{i}\lambda_2 Q_0,\\
&C_5 = (-\mathrm{i}\Delta_2+\kappa_2)+\mathrm{i}\lambda_2 Q_0,\\
&D_1 = C_5(C_0C_1C_2+B_1C_0C_2-B_4C_1C_2),\\
&D_2 = B_1C_0^2C_1C_2C_5,\\
&D_3 = \frac{\mathrm{B}_2C_1C_2+B_3C_5C_0+B_3C_4C_0}{C_4}-C_0C_5+B_4C_5,\\
&D_4 = B_3C_0C_1C_2+B_1C_0^2C_5+\frac{B_3C_0C_1C_2C_5}{C_4},\\
&D_5 = B_3C_0+\frac{C_1C_2B_2+C_0C_5B_3}{C_4},\\
&D_6 = \frac{B_2}{C_4},
\end{aligned} \tag{5}$$

with

$$n_{\mathrm{p}1} = |a_{10}|^2, \quad n_{\mathrm{p}2} = |a_{20}|^2, \quad \alpha_1 = \frac{2\lambda_1^2}{\omega_\mathrm{m}^2}, \quad \alpha_2 = \frac{2\lambda_2^2}{\omega_\mathrm{m}^2},$$

$$\alpha_3 = \frac{2\lambda_1\lambda_2}{\omega_\mathrm{m}^2}, \quad \eta = \frac{\omega_\mathrm{m}^2}{-\delta^2-\mathrm{i}\gamma_\mathrm{m}\delta+\omega_\mathrm{m}^2}.$$

Besides, it is worth noting that we consider the system under the condition of $\omega_\mathrm{m} > \kappa_\mathrm{i}$,[63] so that the NMS can be detected. By utilizing the standard input–output relation: $a_\mathrm{out}(t) = a_\mathrm{in}(t)-\sqrt{2\kappa}a(t)$,[64] the component of the output field oscillating at the probe frequency ω_p can be obtained from

$$\varepsilon_\mathrm{out} = \frac{\sqrt{2\kappa_1}a_{1+}}{E_\mathrm{r}}. \tag{6}$$

In general, the real part $\mathrm{Re}(\varepsilon_\mathrm{out})$ represents the absorption behavior and the imaginary part $\mathrm{Im}(\varepsilon_\mathrm{out})$ describes the dispersion properties of the probe field.[65] Furthermore, for a COMS, the rapid phase dispersion can cause the transmission group delay in the region of the narrow transparency window, which is confirmed as

$$\tau = \frac{\mathrm{d}\phi}{\mathrm{d}t_\mathrm{p}} = \mathrm{Im}\left[\frac{1}{t_\mathrm{p}}\frac{\partial t_\mathrm{p}}{\partial\omega_\mathrm{p}}\right], \tag{7}$$

where $\phi(\omega_\mathrm{p}) = \arg[t_\mathrm{p}(\omega_\mathrm{p})]$ (Refs. [34,66]) is the phase of transmitted field. Correspondingly, the magnitude of group delay is bound up with the rapid phase change in the transmitted probe field. The negative magnitude of the group delay corresponds to fast light propagation, whereas the positive magnitude of the group delay represents slow light propagation. Consequently, it is obvious that the high phase dispersion is always advantageous, causing intensively altered group velocity in the group delay.

3. Optomechanically induced transparency and absorption in the loop-coupled hybrid optomechanical system

In the previous section, we derive the analytic results of the system evolution. In what follows, we numerically illustrate the dependence of the absorption properties of the probe field on the probe–cavity detuning for different system parameters. In order to better comprehend the response of the system to the probe field, the parameters realizable experimentally are chosen as[10] $\omega_\mathrm{m} = 2\pi\times 947$ kHz, $\omega_{\mathrm{c}1} = \omega_{\mathrm{c}2} = 1.77\times 10^{12}$ kHz, $\gamma_\mathrm{m} = 2\pi\times 0.14$ kHz, $\kappa = \kappa_1 = \kappa_2 = 2\pi\times 215$ kHz, and $\lambda = \lambda_1 = \lambda_2 = 250$ Hz.

First of all, we seriously discuss the absorption of the probe field affected by different tunnel coupling strengths in Fig. 2. If two passive optical cavities are weakly coupled for $J < \kappa$, the photon exchange rate is slower than the cavity fields decay rate and there only appears a shallow transparency window around $\Delta_\mathrm{r} = 0$. At this time, the absorption spectrum behaves like OMIT characteristic in a single-mode COMS, where the normal modes are not split and the absorption spectrum of the probe field is mainly caused by the optomechanical interactions. Specifically, the sideband absorption peaks decrease with the increase of tunnel coupling strength J. When the coupling strengths are increased up into the strong regime, *i.e.*, $J > |\kappa_1+\kappa_2|/2 = \kappa$, the photons exchange before the cavity field decays. We obtain that the absorption of the probe spectrum becomes distorted and splits into two normal modes.

This is due to the fact that with the increase of J, the interaction between the two cavities plays a dominant role, which disturbs the absorption spectrum. Compared with Fig. 2(a), it should be pointed out that there exists a rapid transition from absorption dip to peak and at the resonant point in Fig. 2(b). We achieve double transparency windows which are produced by the strong tunnel coupling and the effective optomechanical coupling strengths between the two cavities and the mechanical resonator. Our numerical results also show that the absorption profile reverses from the peak to the dip at $\Delta_r = 0$ when the tunnel coupling is satisfied $J = 4\kappa$. This indicates that the conversion from absorption to amplification can be achieved by adjusting tunnel coupling strength. Specifically, the sideband peaks of absorption appear respectively on the two sides of $\Delta_r = 0$. The distance of the sideband peaks depends linearly on the tunnel coupling J while the heights of them show inversely proportional to J as illustrated in Fig. 3. Therefore, it provides a simple and effective method to measure the tunnel coupling strength by just measuring the distance between the two sideband peaks.

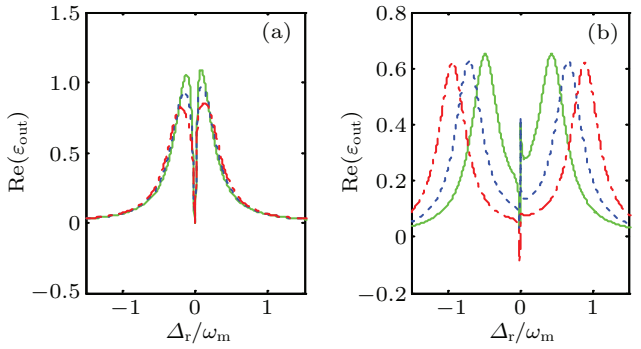


Fig. 2. The real part of the output field $\mathrm{Re}(\varepsilon_{out})$ as a function of the probe–cavity detuning Δ_r/ω_m with different tunnel coupling values. (a) The weak tunnel coupling is given by $J = 0.4\kappa$ (green solid line), $J = 0.6\kappa$ (blue dashed line), $J = 0.8\kappa$ (red dashed-dotted line). (b) The strong tunnel coupling is set as $J = 2\kappa$ (green solid line), $J = 3\kappa$ (blue dashed line), $J = 4\kappa$ (red dashed-dotted line). The corresponding parameter is $E_p = 4\pi$ kHz.

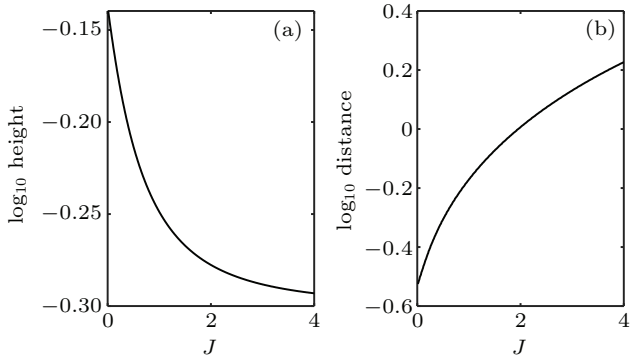


Fig. 3. (a) The logarithm of the heights of two side peaks of absorption varies with the tunnel coupling strengths. (b) The logarithm of the distance between the two side peaks of absorption as a function of the tunnel coupling strength. Other parameters are the same as those in Fig. 2.

In the following, we shall research the effects of the strong pump field with different values when the tunnel coupling is chosen as $J = 2\kappa$. As we known, the effective optomechanical coupling can be enhanced by increasing the driving strength, which can lead to the increase of the mean photon number. In Fig. 4(a), there are two asymmetric sideband peaks. Moreover, the left absorption peak is higher than the right one. Besides, the heights of the two asymmetric absorption peaks is proportional to the driving strength. When the driving strength becomes larger, the left absorption peak moves further away from the resonant point, whereas the right one becomes closer to the point of resonance. In the case of the resonant point, we can see clearly that the absorption is turned into amplification slightly as the driving strength increases. This can be explained by the interaction between photons and phonons. And the quantum interference between the Stokes field and the detection field results in the amplification effect. When the driving amplitude continues to increase, the switch from absorption to amplification appears. As shown in Fig. 4(b), it keeps absorption state for $E_p = 17.08$ kHz but turned into amplification for $E_p = 17.1$ kHz. Due to the stability condition, there exists a critical value for the driving intensity. Further, the absorption properties are very sensitive to the driving strength at $\Delta_r = -\omega_m$. This boundary point gives an idea to get unilateral models for amplifiers.

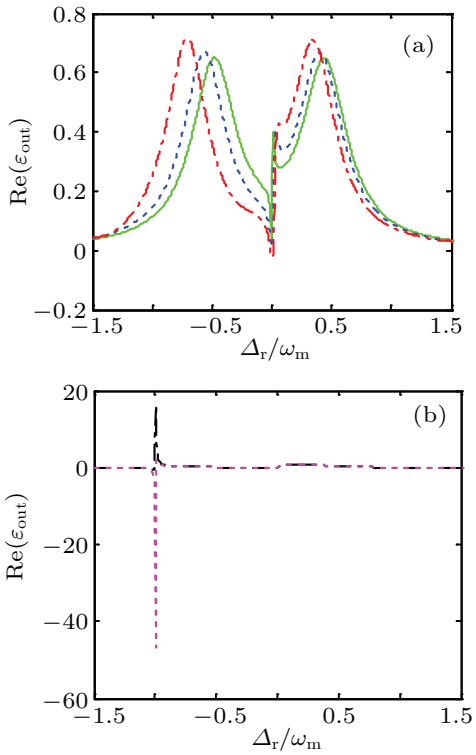


Fig. 4. The real part of the output field $\mathrm{Re}(\varepsilon_{out})$ as a function of probe-cavity detuning Δ_r/ω_m for different driving strengths: (a) $E_p = 4\pi$ kHz (green solid line); $E_p = 8\pi$ kHz (blue dashed line); $E_p = 12\pi$ kHz (red dashed-dotted line); (b) $E_p = 17.08\pi$ kHz (black dashed line); $E_p = 17.1\pi$ kHz (pink dashed-dotted line).

Next, we plot the probe absorption spectrum as a function of Δ_r/ω_m for different decay rates of cavities in Fig. 5. It is found that the distance between the two sideband of the absorption peaks gets larger with the increasing of the cavity

decay. Meanwhile, the sideband peaks of absorption decrease. Likewise, amplification phenomenon can still be found and becomes more obvious with the increase of decay rate.

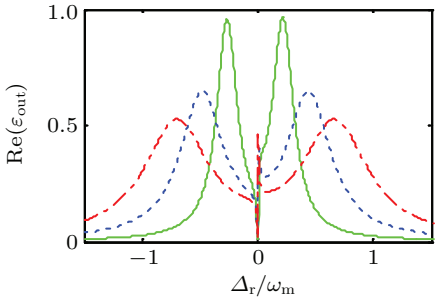


Fig. 5. The real part of the output field $\mathrm{Re}(\varepsilon_{\mathrm{out}})$ as a function of probe–cavity detuning $\Delta_{\mathrm{r}}/\omega_{\mathrm{m}}$ with different κ: $\kappa = \pi \times 215$ kHz, $\kappa = 2\pi \times 215$ kHz, $\kappa = 3\pi \times 215$ kHz for green solid line, blue dashed line, and red dashed-dotted line, respectively. The other parameters are the same as those in Fig. 2.

4. The fast–slow light effects in the loop-coupled hybrid optomechanical system

We have investigated the optomechanically induced transparency and absorption of the loop-coupled hybrid optomechanical system. In what follows, we illustrate the group delay of the probe light as a function of the probe–pump detuning δ with different tunnel coupling J, using the same parameters as in the previous section. Now, we consider the phase dispersion curves of the output probe field. The rapid phase dispersion can generate the transmission group delay. It can be seen clearly from Fig. 6(a) that there is a transparency window combined with a steep negative phase dispersion at the resonant point, which will result in a tunable group delay of the transmitted probe beam.[47] From Fig. 6(b), we obtain that the group delay is positive with a maximum value of 0.57 ms when the tunnel coupling strength is $J = 1.5\kappa$. Further, in the region $J > 2.5\kappa$, the group delay τ becomes negative. The reason for these interesting phenomena is that the fast–slow light effects of the transmitted probe field depend on the phase dissipation of the transmitted probe field, and the phase of the transmitted probe field suffers a fast shift with the change of the tunnel coupling strengths. Therefore, as long as the appropriate value of ω_{m} is selected and the value of J is slightly changed, the regulation of fast and slow light can be realized.

Then, in order to further investigate the effect of optomechanical coupling strengths λ on the fast light and slow light, we present the group delay in Fig. 7. It can be seen by dashed ($\lambda = 250$ Hz) and dashed-dotted ($\lambda = 375$ Hz) curves that the switch between fast light and slow light will occur at the resonant point. Also, the group delay can be further enhanced with different optomechanical coupling strengths and the optimal location moves to left with the increase of the optomechanical coupling strengths. In the hybrid optomechanical system, the pulse advancement can be increased by continuously increasing the optomechanical coupling under a constant tunnel coupling. Hence, we can achieve the high phase dispersion which leads to the higher pulse advancement by employing both coupling parameters.

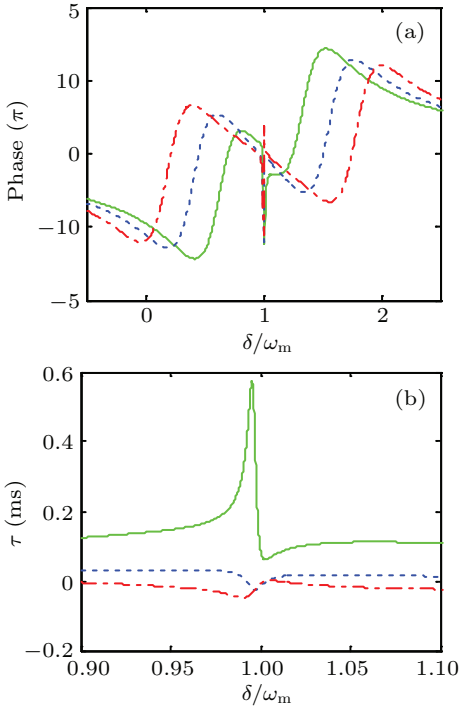


Fig. 6. (a) Phase of the transmission and (b) group delay τ as a function of $\delta/\omega_{\mathrm{m}}$ for different tunneling amplitudes: $J = 1.5\kappa$ (green solid line), $J = 2.5\kappa$ (blue dashed line), $J = 3.5\kappa$ (red dashed-dotted line). We use the other parameters $\lambda = 250$ Hz, $\kappa = 2\pi \times 215$ kHz.

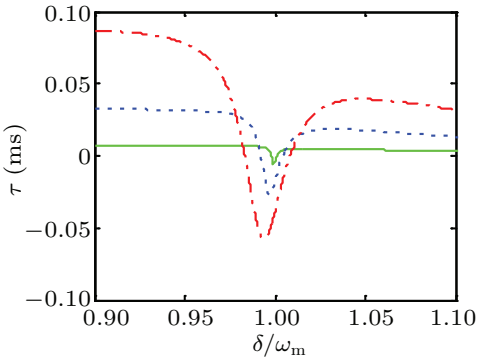


Fig. 7. Group delay τ as a function of $\delta/\omega_{\mathrm{m}}$ for different optomechanical coupling strengths: $\lambda = 125$ Hz (green solid line); $\lambda = 250$ Hz (blue dashed line); $\lambda = 375$ Hz (red dashed-dotted line). Other parameters are the same as those in Fig. 6 besides $J = 2.5\kappa$.

Next, it is natural to wonder how this group delay behaves when $\lambda_1 \neq \lambda_2$. Here, we define $\xi = \lambda_1/\lambda_2$. Figure 8 shows that the output of the probe field maintains slow light in the region of $1 < \xi < 4$, but a conversion from slow light to fast light appears at $\xi = 4.45$. Our numerical results also manifest that, when $\xi > 6$, the influence of ξ on group delay gradually stabilized. Meanwhile, the fast light manifests more obviously. From this figure, we can see that the effect of ξ on group delay is mainly concentrated in $4 < \xi < 6$. Therefore, the tunable slow and fast light effects can be easily realized by adjusting the optomechanical coupling strengths in this optomechanical system.

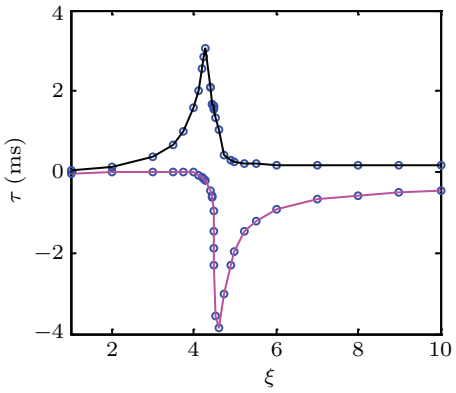


Fig. 8. The maximum (black line) and minimum (pink line) of group delay τ as a function of ξ in the region of $\delta \approx \omega_{\rm m}$. Other parameters are the same as those in Fig. 7.

Finally, it would be interesting to study the influence of the driving strengths $E_{\rm p}$ on the output field group delay which is induced by the mechanical resonator. In Fig. 9, we can see clearly that the group delay converts from positive to negative values and tends to be stable when $\delta/\omega_{\rm m} > 1.05$. We find that the group delay dip becomes shallower and narrower with the decrease of driving strengths. As the driving strength increases, the group delay dip moves further from the resonant point and the group delay is enhanced. At this time, it is accompanied by the transition between fast and slow light. So the adjustability of group delay caused by quantum interference between the probe field and the anti-Stokes field[67] can be dynamically adjusted by controlling the driving field strengths.

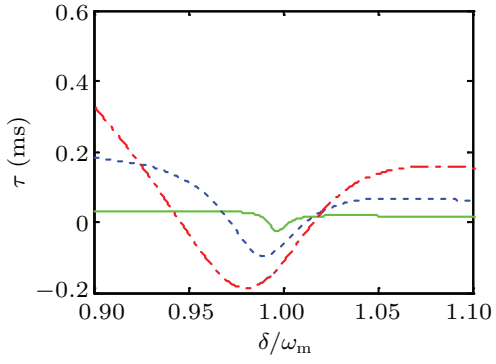


Fig. 9. Group delay τ as a function of $\delta/\omega_{\rm m}$ for different driving strengths: $E_{\rm p} = 4\pi$ kHz (green solid line); $E_{\rm p} = 8\pi$ kHz (blue dashed line); $E_{\rm p} = 12\pi$ kHz (red dashed-dotted line). The other parameters are the same as those in Fig. 6 besides $J = 2.5\kappa$.

5. Conclusion

In conclusion, we have investigated the optomechanically induced transparency of the loop-coupled hybrid system that composes of two optical cavities coupled to a common mechanical resonator for different tunnel couplings. Both OMIT generated by optomechanical interactions and NMS caused by the strong photonic coupling can be observed in this study. We also observed that the amplification phenomenon can occur under the combined action of the optomechanical coupling and the strong tunnel coupling. Furthermore, the intensity and distance of the sideband absorption peaks can be controlled by selecting appropriate parameters. Our research indicates that the conversion between slow light and fast light can also be achieved by modulating optomechanical coupling strengths appropriately. Moreover, the group delay can be enhanced by manipulating the optomechanical coupling strengths. These optical response characteristics can be used to realize the fabrication of optical devices such as the full-photon switch and have a broad application prospect in high-precision measurement and macro-quantum phenomenon research.

References

[1] Aspelmeyer M, Kippenberg T J and Marquardt F 2014 *Rev. Mod. Phys.* **86** 1391
[2] Agarwal G S and Huang S 2012 *Phys. Rev. A* **85** 021810
[3] Horodecki R, Horodecki P, Horodecki M and Horodecki K 2009 *Rev. Mod. Phys.* **81** 865
[4] Vitali D, Gigan S, Ferreira A, Bohm H R, Tombesi P, Guerreiro A, Vedral V, Zeilinger A and Aspelmeyer M 2007 *Phys. Rev. Lett.* **98** 030405
[5] Huang S and Agarwal G S 2009 *Phys. Rev. A* **80** 033807
[6] Hou B P, Wei L F and Wang S J 2015 *Phys. Rev. A* **92** 033829
[7] Chen H J, Yang J Y, Wu H W and Li X C 2019 *Eur. Phys. J. D* **73** 206
[8] Lai D G, Huang J F, Yin X L, Hou B P, Li W L, Vitali D, Nori F and Liao J Q 2020 *Phys. Rev. A* **102** 011502
[9] Marquardt F, Chen J P, Clerk A A and Girvin S M 2007 *Phys. Rev. Lett.* **99** 093902
[10] Riviere R, Deleglise S, Weis S, Gavartin E, Arcizet O, Schliesser A and Kippenberg T J 2011 *Phys. Rev. A* **83** 063835
[11] Teufel J D, Donner T, Li D, Harlow J W, Allman M S, Cicak K, Sirois A J, Whittaker J D, Lehnert K W and Simmonds R W 2011 *Nature* **475** 359
[12] Fleischhauer M, Imamoglu A and Marangos J P 2005 *Rev. Mod. Phys.* **77** 633
[13] Lü H, Wang C Q, Yang L and Jing H 2018 *Phys. Rev. Appl.* **10** 014006
[14] Li D K, Ma Y W, Chen Z H, Qian H W and Ning R X 2020 *Opt. Quantum Electron.* **52** 253
[15] Harris S E 1997 *Phys. Today* **50** 36
[16] Akram M J, Ghafoor F and Saif F 2015 *J. Phys. B: At. Mol. Opt. Phys.* **48** 065502
[17] Andersson G, Ekstrom M K and Delsing P 2020 *Phys. Rev. Lett.* **124** 240402
[18] Qu K and Agarwal G S 2013 *Phys. Rev. A* **87** 031802
[19] Yan X B 2020 *Phys. Rev. A* **101** 043820
[20] Karuza M, Biancofiore C, Bawaj M, Molinelli C, Galassi M, Natali R, Tombesi P, Giuseppe G D and Vitali D 2013 *Phys. Rev. A* **88** 013804
[21] Zhang X Y, Zhou Y H, Guo Y Q and Yi X X 2018 *Phys. Rev. A* **98** 033832
[22] Xia W Q, Yu Y F and Zhang Z M 2017 *Chin. Phys. B* **26** 054210
[23] Monroe C 2002 *Nature* **416** 238
[24] Braunstein S L and Pati A K 2003 *Rev. Mod. Phys.* **77** 513
[25] Zheng M H, Wang T, Wang D Y, Bai C H, Zhang S, An C S and Wang H F 2019 *Sci. China-Phys. Mech.* **62** 950311
[26] Agarwal G S and Huang S 2010 *Phys. Rev. A* **81** 041803
[27] Huang S and Agarwal G S 2011 *Phys. Rev. A* **83** 043826
[28] Safavinaeini A H, Alegre T P, Chan J, Eichenfield M, Winger M, Lin Q, Hill J T, Chang D E and Painter O 2011 *Nature* **472** 69
[29] Safavinaeini A H, Alegre T P, Winger M and Painter O 2010 *Appl. Phys. Lett.* **97** 181106
[30] Liao J Q and Nori F 2013 *Phys. Rev. A* **88** 023853
[31] Lü H, Jiang Y J, Wang Y Z and Jing H 2017 *Photon. Res.* **5** 367
[32] Jing H, Ozdemir S K, Geng Z, Lü X Y, Peng B, Yang L and Nori F 2015 *Sci. Rep.* **5** 9663
[33] Jing H, Özdemir S K, Lü X Y, Zhang J, Yang L and Nori F 2014 *Phys. Rev. Lett.* **113** 053604
[34] Chen B, Jiang C and Zhu K D 2011 *Phys. Rev. A* **83** 055803
[35] Liu Y C, Li B B and Xiao Y F 2017 *Nanophotonics: Berlin* **6** 789
[36] Xiong H and Wu Y 2018 *Appl. Phys. Rev.* **5** 031305

[37] Wang B, Liu Z X, Kong C, Xiong H and Wu Y 2019 *Opt. Express* **27** 8069
[38] Thevenaz L 2008 *Nat. Photon.* **2** 474
[39] Tarhan D, Huang S and Mustecaploglu O Z E 2013 *Phys. Rev. A* **87** 013824
[40] Ziauddin, Rahmatullah, Hussain A and Abbas M 2020 *Opt. Commun.* **461** 125284
[41] Liao Q H, Xiao X, Nie W J and Zhou N R 2020 *Opt. Express* **28** 5288
[42] Fleischhauer M, Imamoglu A and Marangos J P 2005 *Rev. Mod. Phys.* **77** 633
[43] Zhan X G, Si L G, Zheng A S and Yang X X 2013 *J. Phys. B* **46** 025501
[44] Akram M J, Khan M M and Saif F 2015 *Phys. Rev. A* **92** 023846
[45] Boyd R W and Gauthier D J 2009 *Science* **326** 1074
[46] Wu Z, Luo R H, Zhang J Q, Wang Y H, Yang W and Feng M 2017 *Phys. Rev. A* **96** 033832
[47] Jiang C, Liu H X, Cui Y S, Li X W, Chen G B and Chen B 2013 *Opt. Express* **21** 12165
[48] Macke B and Segard B 2020 *J. Opt. Soc. Am. B* **37** 2080
[49] Chen H J 2020 *Eur. Phys. J. D* **74** 118
[50] Xu W L, Gao Y P, Cao C, Wang T J and Wang C 2020 *Phys. Rev. A* **102** 043519
[51] Hao H, Kuzyk M C, Ren J J, Zhang F, Duan X K, Zhou L, Zhang T C, Gong Q H, Wang H L and Gu Y 2019 *Phys. Rev. A* **100** 023820
[52] Zhao W, Zhang S D, Miranowicz A and Jing H 2020 *Sci. China-Phys. Mech.* **63** 224211
[53] Lai D G, Wang X, Qin W, Hou B P, Nori F and Liao J Q 2020 *Phys. Rev. A* **102** 023707
[54] Liu L, Hou B P, Zhao X H and Tang B 2019 *Opt. Express* **27** 008361
[55] Lai D G, Zou F, Hou B P, Xiao Y F and Liao J Q 2018 *Phys. Rev. A* **98** 023860
[56] Qian Z, Zhao M M, Hou B P and Zhao Y H 2017 *Opt. Express* **25** 33097
[57] Bai C, Hou B P, Lai D G and Wu D 2016 *Phys. Rev. A* **93** 043804
[58] Ludwig M, Safavinaeini A H, Painter O and Marquardt F 2012 *Phys. Rev. Lett.* **109** 063601
[59] Komar P, Bennett S D, Stannigel K, Habraken S J M, Rabl P, Zoller P and Lukin M D 2013 *Phys. Rev. A* **87** 013839
[60] Jiang C, Chen B and Zhu K D 2011 *J. Europhys. Lett.* **94** 38002
[61] Paraiso T K, Kalaee M, Zang L Y, Pfeifer H, Marquardt F and Painter O 2015 *Phys. Rev. X* **5** 041024
[62] Gan J H, Liu Y C, Lu C C, Wang X, Tey M K and You L 2019 *Laser Photon. Rev.* **13** 1900120
[63] Vitali D, Tombesi P, Woolley M J, Doherty A C and Milburn G J 2007 *Phys. Rev. A* **76** 042336
[64] Yellapragada K C, Pramanik N, Singh S and Lakshmi P A 2018 *Phys. Rev. A* **98** 053822
[65] Wang H, Gu X, Liu Y X, Miranowicz A and Nori F 2014 *Phys. Rev. A* **90** 023817
[66] Jiang C, Cui Y S, Zhai Z Y, Yu H L, Li X W and Chen G B 2018 *Opt. Express* **26** 28834
[67] Wei W Y, Yu Y F and Zhang Z M 2018 *Chin. Phys. B* **27** 034204